Int. J. Multiphase Flow Vol. 16, No. 3, pp. 363–374, 1990
Printed in Great Britain

0301-9322/90 $3.00 + 0.00
Pergamon Press/Elsevier

RATES OF ATOMIZATION AND DEPOSITION IN VERTICAL ANNULAR FLOW

S. A. SCHADEL,[1] G. W. LEMAN,[1] J. L. BINDER[2] and T. J. HANRATTY[1]
Departments of [1]Chemical and [2]Nuclear Engineering, University of Illinois, Urbana, IL 61801, U.S.A.

(*Received* 23 *November* 1988; *in revised form* 23 *January* 1990)

Abstract—The tracer technique of Quandt has been used to determine the rate of atomization, the rate of deposition and the entrainment for air and water flowing vertically upward in 2.54, 4.20 and 5.72 cm pipes. The rate of atomization was found to vary linearly with gas velocity and liquid film flow rate. The rate of deposition varies linearly with droplet concentration at low concentrations but is insensitive to changes in droplet concentration at high concentrations.

Key Words: annular flow, atomization, deposition, entrainment

1. INTRODUCTION

For the annular regime, that exists when gas and liquid flow in a vertical pipe, part of the liquid moves along the wall as a liquid film and part as droplets in the high velocity gas (Hewitt & Hall-Taylor 1970). At very low liquid throughputs the thin liquid wall film is covered with small capillary ripples. Above a certain liquid film flow rate (Dallman *et al.* 1979; Andreussi *et al.* 1985) there are large amplitude surges in the film flow rate, called roll waves or disturbance waves. Atomization has been observed to occur by the removal of small waves that ride on the top of these disturbance waves (Woodmansee & Hanratty 1969).

The critical problem in analyzing annular flows is the prediction of the fraction of the liquid flowing as droplets; that is, entrainment, E. The entrainment is the consequence of two rate processes: the rate of atomization of the liquid film, R_A; and the rate of deposition of droplets on to the film, R_D. For long enough pipes a fully-developed condition is reached where an equilibrium between atomization and deposition occurs, $R_A = R_D$.

A number of comprehensive studies of entrainment have been carried out (Asali *et al.* 1985a; Owen *et al.* 1985). None of these have produced satisfactory correlations. It is now generally accepted that the correct way to obtain predictive methods for E is to develop theoretical understanding and correlations for the basic rate processes. Such an approach will not only give better predictions for fully-developed conditions but also will offer the opportunity to deal with nonequilibrium developing flows.

This paper presents the results of a comprehensive study of R_A and R_D for upward flow of air and water that defines the effect of liquid flow rate, gas flow rate and pipe diameter. The experiments were in the same equipment as used in previous studies by Asali (1984) and Leman (1985). Consequently, data are available for the system studied on the entrainment (Asali *et al.* 1985a) and the pressure drop (Asali *et al.* 1985b).

The tracer technique, originally developed by Quandt (1965) and later improved by Andreussi & Zanelli (Andreussi & Zanelli 1976; Andreussi 1983) was used. A continuous supply of a salt solution was injected into the film at a location where the flow is fully developed. The concentration of salt in the film is measured at different distances downstream from the point of injection. Mass balances can then be used to relate these measurements to the rate of interchange between the film and the initially unsalted droplets in the gas.

Details regarding the application of this technique in the experiments reported in this paper are given in theses by Leman (1985) and Schadel (1988). In initial experiments samples of the film were withdrawn through a porous wall and analyzed for salt content. In later work the salt concentration was determined *in situ* by measuring its concentration with two conductance probes mounted flush with the wall. The conductivity of the film depends on the film height and wave structure, as well

as the salt concentration. Therefore, in using the *in situ* method it was necessary to calibrate the conductance probes for each flow condition studied.

In many experiments significant differences in results obtained by the two methods were obtained. These could be associated with disturbances in the film caused by withdrawing samples. Consequently, only results obtained with the *in situ* method are reported in this paper. The experiments were conducted in pipes with diameters of 2.54, 4.20 and 5.72 cm. Air velocities ranging from 20 to 120 m/s and liquid fluxes of 1.20–10.0 g/s cm^2 were investigated.

2. ESTIMATION OF DROPLET RELATIVE VELOCITY

A rate law for droplet deposition is defined as

$$R_D = k_D C_D, \tag{1}$$

where C_D is the droplet concentration expressed as mass per unit volume. However, in studies of droplet deposition the mass flow rate of entrained drops, W_{LE}, is measured instead of C_D. Thus, rate law [1] can be written as

$$R_D = k_D \frac{4\,W_{LE}}{\pi D^2 U_G S}, \tag{2}$$

where D is the pipe diameter, U_G is the gas velocity and S is the ratio of the drop velocity to the gas velocity,

$$S = \frac{U_P}{U_G}. \tag{3}$$

Usually S is not known so the rate law is written as

$$R_D = k \frac{4\,W_{LE}}{\pi D^2 U_G}, \tag{4}$$

where

$$k = \frac{k_D}{S}. \tag{5}$$

No direct measurements of S were made in this study. Therefore, to determine the effect of S it was necessary to carry out an approximate calculation. The gas velocity was assumed to be uniform over the cross section of the pipe. The droplets were assumed to enter the gas flow at a streamwise velocity of U_{P0} which is, following the suggestion of Moeck & Stachiewicz (1972), taken as the velocity of the liquid at the interface of the liquid (roughly the roll wave velocity).

The change of the velocity of the droplets with time is given by

$$\frac{dU_P}{dt} = \frac{3}{4}\frac{C_D}{d_P}\frac{\rho_G}{\rho_L}(U_G - U_P)^2 - g \tag{6}$$

for vertical upward flow. For the range of conditions [U_G = 20–116 m/s; d_P = 21–171 μm] used in this study the particle Reynolds number, defined as

$$Re_P = \frac{(U_G - U_P)\,d_P}{\nu_G} = \frac{U_G(1 - S)\,d_P}{\nu_G}, \tag{7}$$

varies between 41 and 141. A drag coefficient equation valid for intermediate Reynolds numbers,

$$C_D = \frac{18.5}{Re_P^{0.6}}, \tag{8}$$

should be used in [6].

Equation [6] was solved numerically for the particle velocity with a fourth-order Runge–Kutta method for a given initial velocity U_{P0} at time zero. This calculated $U_P(t)$ was integrated numerically to calculate the distance traveled, η, for a given residence time of a particle in the field.

Consider a location $z = 0$ in the fully-developed region. Define $F(z)\,dz$ as equal to the fraction of the droplets which originated from a location upstream between z and $z + dz$. Thus,

$$W_{LE} = \int_0^\infty F(z)\, R_A\, \pi D\, dz. \qquad [9]$$

The average droplet velocity at $z = 0$ is given as

$$\bar{U}_P = \frac{\int_0^\infty U_P(z)\, F(z)\, dz}{\int_0^\infty F(z)\, dz}, \qquad [10]$$

where $U_P(z) = U_P(\eta)$ is obtained from the numerical integration of [6].

Experimental results to be presented in section 5 show that for low droplet concentrations R_D varies linearly with W_{LE} and that for very high droplet concentrations R_D is approximately independent of W_{LE}. For the case of a rate of deposition that is linearly dependent on W_{LE},

$$R_D = k\frac{4\,W_{LE}}{\pi D^2} \qquad [11]$$

and

$$F_1(z) = \exp\left(-\frac{R_D \pi D}{W_{LE}} z\right). \qquad [12]$$

For the case of $R_D = \text{const}$,

$$F_2(z) = \begin{cases} 1 - \dfrac{z\, R_D\, \pi D}{W_{LE}}, & z < \dfrac{W_{LE}}{R_D \pi D} \qquad [13] \\ 0, & z > \dfrac{W_{LE}}{R_D \pi D}. \qquad [14] \end{cases}$$

For cases between these two limiting behaviors it is convenient to take

$$F(z) = \exp(-\lambda C_D)\, F_1(z) + [1 - \exp(-\lambda C_D)]\, F_2(z), \qquad [15]$$

where λ is an empirically determined constant.

3. DESCRIPTION OF THE EXPERIMENTS

(a) Flow loop

A schematic of the flow loop in which the experiments were conducted is given in figure 1. Detailed descriptions may be found in theses by Asali (1984) and Leman (1985). Water was fed to the system from the municipal supply through a slotted entry that introduced the liquid along the wall of the pipe as an annular layer. A length of pipe >150 tube diameters preceded the test section. The lengths of the test sections were 25, 24 and 65 pipe diameters for the 2.54, 4.20 and 5.72 cm pipes, respectively.

(b) Tracer technique

The test section consisted of a tracer injection port followed by a minimum of six conductance probes that covered its entire length. The tracer was a 15 wt%/aqueous solution of sodium chloride. A brief description of the injectors and the conductance probes is given below. A detailed description of the test sections can be found in the thesis by Schadel (1988).

The injector consisted of two rows of rectangular slits around the pipe circumference that are separated by a distance of 0.05 cm. These slits were staggered so that the salt solution was uniformly distributed around the circumference. This injector was tested in a series of experiments for a liquid film flowing down the pipe with no air flow, and therefore no entrained drops. The concentration of salt was found to be the same for all of the measurement stations.

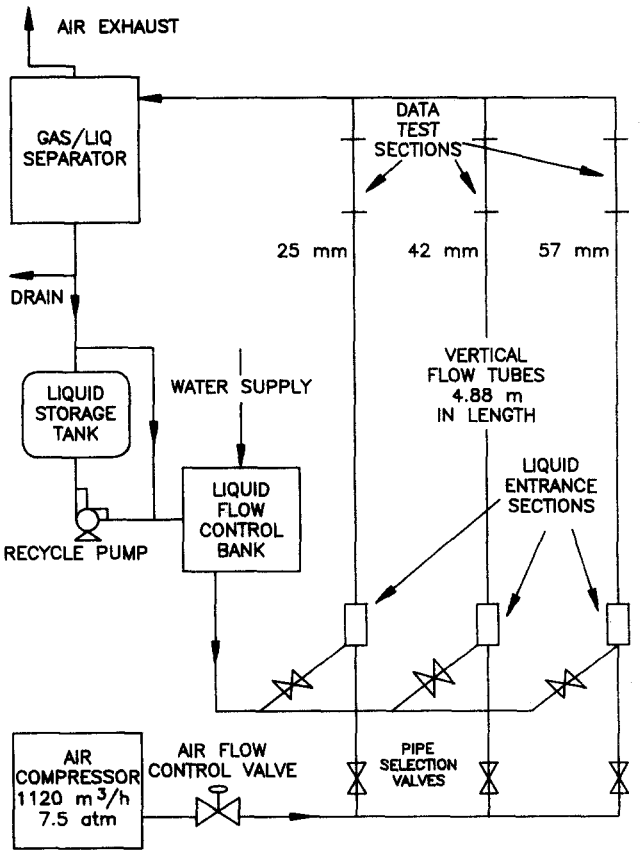

Figure 1. Schematic of the flow loop.

Each conductance probe consisted of two stainless-steel flush-mounted ring electrodes, 0.30 cm long, which circle the entire pipe. These electrodes were separated with a 0.20 cm long Plexiglas spacer.

A 100 kHz voltage was applied to a pair of the electrodes. The measured current was demodulated [using a circuit described by Andritsos (1986)] to give an analog signal which is related to the conductance of the film between the electrodes. This relationship was determined for each probe pair by a static calibration.

A second *in situ* calibration was also performed for each experiment to determine the relationship of film conductivity to salt concentration for the particular wave pattern that existed. This was done

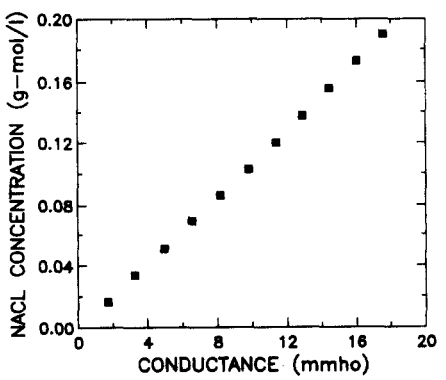

Figure 2. Typical calibration curve for the conductance meter.

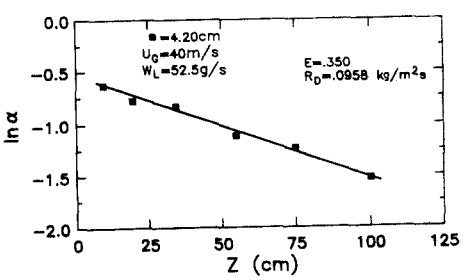

Figure 3. Plot illustrating the analysis of the measurements to obtain exchange rates.

by injecting a small known amount of tracer into the water supply line, so that the salt concentration of all of the liquid was the same at the test section. By injecting different amounts of tracer the concentration could be varied. A typical calibration curve for one of the electrode pairs is shown in figure 2, where the conductivity is the time-averaged value.

4. ANALYSIS OF MEASUREMENTS

The analysis of the data follows procedures discussed by Andreussi & Zanelli (1976) and by Leman *et al.* (1984).

A mass balance on the liquid gives

$$\frac{dW_{LF}}{dz} = \pi D(R_D - R_A), \qquad [16]$$

where W_{LF} is the mass flow rate of the liquid film, D is the pipe diameter and z is the coordinate in the direction of mean flow. If the salt is assumed to be uniformly mixed in the film and in the droplets in the gas flow, a mass balance on the salt gives

$$\frac{d(W_{LF} C_F)}{dz} = \pi D\,(R_D C_D - R_A C_F), \qquad [17]$$

where C_F is the concentration of the salt in the film and C_D is the concentration in the entrained liquid.

By subtracting the product of C_F and [16] from [17], the following result is obtained:

$$\frac{dC_F}{dz} = -\frac{\pi D}{W_{LF}}(C_F - C_D)\,R_D. \qquad [18]$$

The mass balance relation can be used to eliminate C_D from [18]:

$$C_F(1-E) + C_D\,E = C_{MC}, \qquad [19]$$

where C_{MC} is the mixing cup concentration which was determined for each measurement with a pair of wall electrodes by taking a liquid sample from the separator. From [18] and [19] it follows that

$$\frac{d\ln\alpha}{dz} = -\frac{\pi D\,R_D}{W_L}\frac{1}{E(1-E)}, \qquad [20]$$

where

$$\alpha = \frac{C_F - C_{MC}}{C_{MC}}. \qquad [21]$$

Equation [20] indicates that a plot of ln α vs z yields a straight line with slope m, where

$$m = -\frac{\pi D\,R_D}{W_L\,E(1-E)}. \qquad [22]$$

The intercept at $z = 0$ gives $(C_{F0} - C_{MC})/C_{MC}$, which can be used to calculate E from [19], since $C_{A0} = 0$:

$$\frac{C_{F0} - C_{MC}}{C_{MC}} = \frac{E}{1-E}. \qquad [23]$$

Therefore R_D and E can be determined from measurements of $C_F(z)$ by using [22] and [23].

Figure 3 shows a typical plot of ln α vs z. In initial work in which a perforated entry was used for the salt solution and in which samples of the wall film were withdrawn a linear relation between ln α and z was not always obtained. The slope tended to be larger for small z, as was observed by Andreussi (Andreussi & Azzopardi 1983; Andreussi 1983).

The assumption of a uniform concentration in the film is supported by experiments with a downward flowing film, cited in the previous section, and by the work of Andreussi & Zanelli (1976). However, the assumption that the concentration of the depositing drops is given by [19]

is still open to question. Therefore, a simplified analysis was also used which is strictly valid for small z where $C_D \approx 0$. In this case [18] and [19] give

$$\frac{d \ln\left(\frac{C_F}{C_{MC}}\right)}{dz} = -\frac{\pi D}{W_L(1-E)} R_D. \quad [24]$$

Thus, a plot of ln (C_F/C_{MC}) vs z should yield a straight line for small z whose slope is given by

$$n = -\frac{\pi D}{W_L(1-E)} R_D. \quad [25]$$

Again, the entrainment can be calculated from the intercept of such a plot with [23].

Schadel (1988) explored both methods and found no significant difference in the values of E and R_D that were determined.

5. RESULTS

(a) Critical film flow rates

A typical plot of R_A vs the liquid flow rate W_L is shown in figure 4. It is noted that the results can be fitted with a straight line. The extrapolation of this line to $R_A = 0$ yields a critical flow below which atomization does not occur, W_{LFC}. Values of this critical flow expressed in units of mass per unit time per unit of circumferential length, $\Gamma_0 = W_{LFC}/\pi D$, are summarized in table 1.

Asali *et al.* (1985a) determined W_{LFC} by plotting the liquid film flow rate, W_{LF}, vs gas velocity for a fixed liquid flow W_L. At large gas velocities the plot reached a minimum film flow, which was defined as W_{LFC}. In this way critical flow rates of 5.6 and 10 g/s were determined for air–water flows in 2.29 and 4.20 cm pipes, respectively. It is noted that these are in approximate agreement with the values presented in table 1.

The method used in present paper has advantages over that used by Asali *et al.* (1985), in that it enables a determination of the effect of the gas velocity on W_{LFC} and that it is simpler and more straightforward.

(b) The rate of atomization

Measurements of the rate of atomization are plotted in figures 5–7 for the three different pipe diameters studied. The ordinate is a dimensionless R_A, defined as

$$\tilde{R}_A = \frac{R_A}{U_G(\rho_G \rho_L)^{1/2}}. \quad [26]$$

The abscissa is the excess film flow rate per unit of circumferential length, $\Gamma - \Gamma_0$, in units of kg/ms.

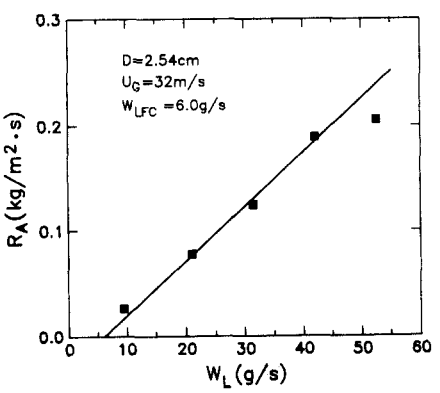

Figure 4. The determination of the critical flow rate of the liquid film.

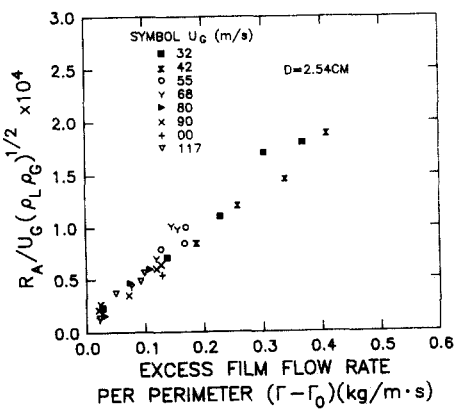

Figure 5. Rates of atomization measured in the 2.54 cm tube.

Table 1. Critical liquid flow rates

			D = 2.54 cm				
$U_G\left[\frac{m}{s}\right]$	32	55	68	80	89	99	115
$W_{LFC}\left[\frac{g}{s}\right]$	6.0	5.6	4.9	4.9	4.9	4.9	5.0
$\Gamma_o = \frac{W_{LFC}}{\pi D}\left[\frac{kg}{m \cdot s}\right]$	0.0752	0.072	0.0614	0.0614	0.0614	0.0614	0.0627
$Re_{LFC} = \frac{4W_{LFC}}{\pi D\mu}$	259	242	212	212	212	212	216
			D = 4.20 cm				
$U_G\left[\frac{m}{s}\right]$	19.5	36.5	53.0	72.0			
$W_{LFC}\left[\frac{g}{s}\right]$	11.7	12.0	9.0	9.3			
$\Gamma_o\left[\frac{kg}{n \cdot s}\right]$	0.0887	0.0909	0.0682	0.0705			
RE_{LFC}	306	314	235	243			
			D = 5.715 cm				
$U_G\left[\frac{m}{s}\right]$	25	33	41	49			
$W_{LFC}\left[\frac{g}{s}\right]$	23.5	23.5	14.4	14.4			
$\Gamma_o\left[\frac{kg}{m \cdot s}\right]$	0.131	0.131	0.0801	0.0801			
Re_{LFC}	451	451	276	276			

It is noted that all of these plots are fitted quite well with a linear relation

$$\tilde{R}_A = k_A(\Gamma - \Gamma_o), \qquad [27]$$

with

$$k_A = 4.97 \times 10^{-4}\,\text{ms/kg}, \quad D = 2.54\,\text{cm},$$
$$k_A = 4.36 \times 10^{-4}\,\text{ms/kg}, \quad D = 4.20\,\text{cm},$$

and

$$k_A = 4.33 \times 10^{-4}\,\text{ms/kg}, \quad D = 5.72\,\text{cm}.$$

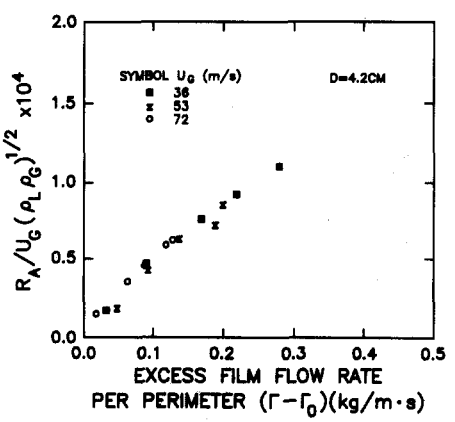

Figure 6. Rates of atomization measured in the 4.20 cm tube.

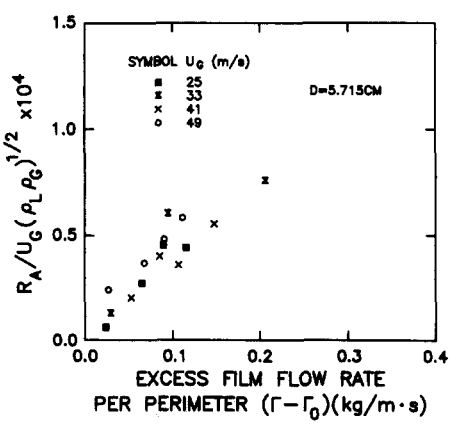

Figure 7. Rates of atomization measured in the 5.715 cm tube.

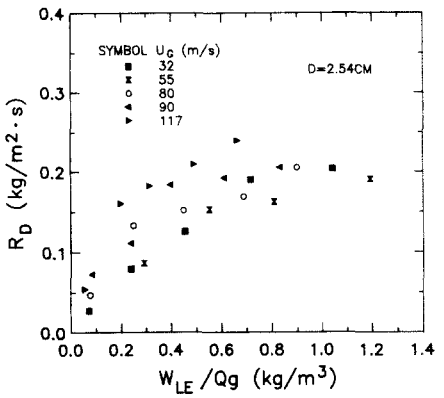

Figure 8. Rates of deposition measured in the 2.54 cm tube.

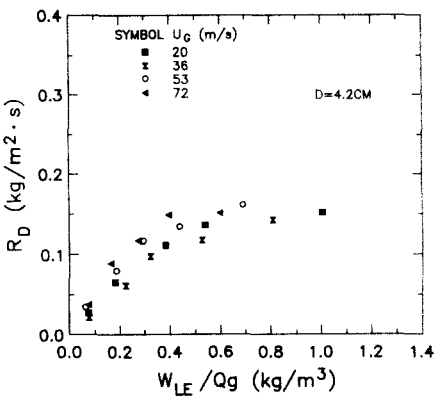

Figure 9. Rates of deposition measured in the 4.20 cm tube.

The average of all data points is $k_A = 4.70 \times 10^{-4}$ ms/kg. For the range of variables studied k_A is independent of pipe diameter and gas velocity.

Dallman *et al.* (1979) developed the following relation from measurement in tubes with diameters of 9.5 and 12.6 mm by Cousins & Hewitt (1968) and by Hinkle (1967):

$$\tilde{R}_A = k'_A U_G(\Gamma - \Gamma_\circ), \qquad [28]$$

with $k'_A = 6.7 \times 10^{-6}$ s^2/kg. This study confirms the suggestion of Dallman *et al.*, that R_A varies linearly with $(\Gamma - \Gamma_\circ)$. However, the effect of gas velocity is observed to be different from what was observed in small diameter tubes. The observation that R_A varies linearly with U_G is more consistent with the results of Andreussi & Zanelli (1979) for downward flow of air and water in a 24 mm tube.

(c) Rates of deposition

Measurements of the rate of deposition are presented in figures 8–10. The abscissa in these plots is the ratio of the mass flow of entrained liquid to the volumetric flow of gas, W_{LE}/Q_G. If the drops were moving at the same velocity as the gas this would equal the droplet concentration.

For small droplet concentrations the rate of deposition varies roughly linearly with W_{LE}/Q_G, as would be expected. The most surprising aspect of these measurements is that for droplet concentrations $\gtrsim 0.6$ kg/m^3, R_D appears to be roughly independent of droplet concentration. It should be recognized that $W_{LE}/Q_G = $ kg/m^3 would correspond to a time-averaged volume fraction of liquid in the gas of only 0.001.

Another aspect of these results which seems difficult to explain is that they are relatively insensitive to changes in the gas velocity. Thus, the results in figures 8–10 are represented by

$$R_D = \frac{0.034}{D^{0.6}} \frac{W_{LE}}{Q_G} \left[\frac{\text{kg}}{\text{m}^2\text{s}}\right], \qquad [29]$$

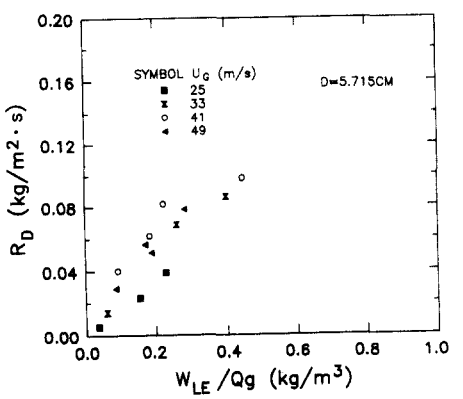

Figure 10. Rates of deposition measured in the 5.715 cm tube.

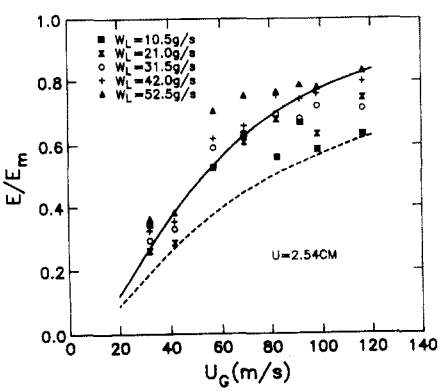

Figure 11. Entrainment measurements made in the 2.54 cm tube.

for $W_{LE}/Q_G \leqslant 0.078/D^{0.6}$ kg/m^3, and by

$$R_D \cong \frac{0.021}{D^{0.6}} \left[\frac{\text{kg}}{\text{m}^2\text{s}}\right], \qquad [30]$$

for $W_{LE}/Q_G > 0.078/D^{0.6}$ kg/m^3.

Other investigators have observed that k decreases with W_{LE}/Q (Namie & Ueda 1972; Andreussi & Azzopardi 1983). In particular, it is interesting to note that the measurements of k reported by Andreussi & Azzopardi (1983) vs W_{LE}/Q_G are approaching an asymptotic behavior of $k \sim (W_{LE}/Q_G)^{-1}$ at large W_{LE}/Q_G.

(d) Entrainment

Entrainment measurements are presented in figures 11–13 as E/E_{max}. Here E_{max} is the maximum amount of entrainment attainable,

$$E_{max} = \frac{W_L - W_{LFC}}{W_L}. \qquad [31]$$

The entrainment ratio, E/E_{max}, is more sensitive to changes in the gas velocity than to changes in the liquid flow rate. It increases with increasing gas velocity and with increasing liquid flow rate.

6. DISCUSSION

(a) Rate of atomization

The correlation of the measurements of the rate of atomization with [27] is quite good. In particular, it is noted that k_A is independent of pipe diameter and gas velocity. However, since this is an empirical correlation it would be dangerous to apply it for conditions that are quite different from those used in this study.

The units of k_A are the same as the viscosity and Γ_o/μ_L is approximately constant. Therefore, it is tempting to argue that k_A varies inversely with μ_L. However, this type of correlation would suggest a much stronger effect of liquid viscosity on entrainment than was found in the measurements of Asali *et al.* (1985a).

The theory of Taylor (Schadel & Hanratty 1989), based on a Kelvin–Helmholtz wave growth mechanism, suggests that R_A is correlated as

$$\tilde{R}_A = f\left(\rho_G U_G^2 \frac{\lambda}{\sigma}\right) \qquad [32]$$

for liquids that are not too viscous. Here λ is the wavelength of the atomizing wave and σ is the surface tension. For deep liquids the Weber number is constant and $\tilde{R}_A$ is a constant, N. Since, for annular flows, atomization does not occur over the whole surface of the liquid layer but only from the top of roll wave, this type of argument suggests that

$$\tilde{R}_A = I\,\text{N}, \qquad [33]$$

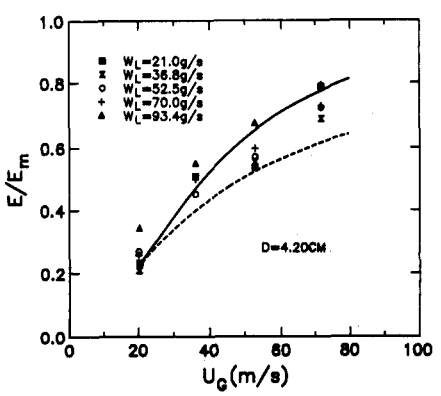

Figure 12. Entrainment measurements made in the 4.20 cm tube.

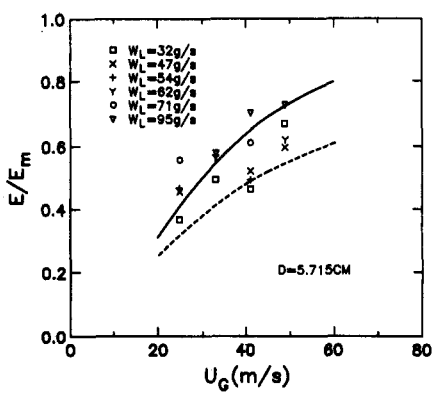

Figure 13. Entrainment measurements made in the 5.715 cm tube.

where intermittency, I, is the fraction of time when roll waves are present. A comparison of [33] and [27] then provides the interpretation that $(\Gamma - \Gamma_o)$ is proportional to I.

Schadel & Hanratty (1988) have reported detailed measurements of wave properties. It is found that I is not proportional to $(\Gamma - \Gamma_o)$. An equation of the form of [32] is consistent with the measurements of R_A if λ is assumed proportional to the height of the roll waves and if the intermittent presence of the roll waves is taken into account. This type of theoretical interpretation suggests that k_A increases with increasing surface tension and is rather insensitive to variations of liquid viscosity. More measurements with liquids other than water are needed to check this interpretation.

(b) Rate of deposition

The results on the rate of deposition given by [29] and [30] are surprising in that R_D is approximately independent of the gas velocity. Furthermore, the dependence of k on the pipe diameter is not easily explained. From [5] it is noted that $k = k_D/S$. The poorly understood behavior of k leads to a consideration that the relative velocity, S, is not constant and that much of the observed behavior of k could be reflecting variations of S. Both Moeck & Stachiewicz (1972) and Andreussi & Zanelli (1976) have explored this previously.

Values of the relative velocity ratio calculated by the method outlined in section 2 [using the drop size measurements of Azzopardi (1988)] are shown in figure 14. These relative velocity ratios were then used to calculate droplet concentrations from measured W_{LE}. The measurements of R_D plotted vs C_D show a much stronger effect of gas velocity than is indicated in figures 8–10, where R_D is plotted vs W_{LE}/Q_G.

Figure 15 shows the ratio of R_D to the friction velocity plotted vs C_D. This type of correlation appears relatively insensitive to pipe diameter and to gas velocity. It should be noted that the friction velocity used in figure 15 is based on the interfacial friction factor determined from the pressure drop measurements under actual annular flow conditions by Asali *et al.* (1985b). For $C_D \to 0$ it is noted that $k_D/u_i^* = 0.10$. If the friction factor for a smooth surface were used, then a value of $k_D/u_s^* = 0.12$ is obtained for $C_D \to 0$. The conclusion is that k_D is independent of pipe diameter and varies linearly with friction velocity.

The above results indicate that the interpretation of deposition measurements at small concentrations is possible through the use of diffusion concepts, as outlined by Lee *et al.* (1989) and Andreussi & Azzopardi (1983). However, the decrease of k_D/C_D at large C_D is not understood. Two possibilities are that droplet size increases with increasing concentration and that the presence of droplets dampens gas-phase turbulence.

Increases in droplet size with increasing drop concentration have been noted by Teixeira *et al.* (1987). This could cause a decrease in the ability of drops to follow the gas-phase turbulence and, therefore, a decrease in the deposition rate. A damping of gas-phase turbulence by droplets was suggested by Namie & Ueda (1972) to interpret their measurements of droplet deposition rates. This idea has been pursued by a number of investigtors, including Abolfadl & Wallis (1985), Owen & Hewitt (1987), Azzopardi (1988) Hewitt *et al.* (1964).

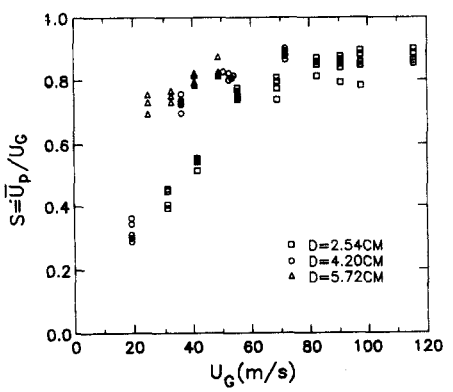

Figure 14. Calculated relative velocities.

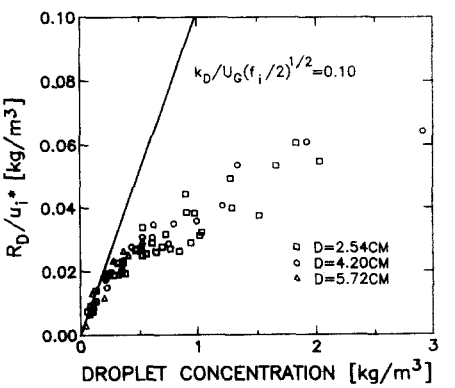

Figure 15. Rates of deposition correlated against droplet concentration.

(c) Entrainment

The important role of entrainment in analyzing the performance of annular flow systems has lead to the development of a number of correlations for fully-developed flow. It is therefore worthwhile to examine the relevance of the measurements presented in this paper to the prediction of entrainment under this limiting condition.

Dallman *et al.* (1979) suggested that entrainment data be plotted as E/E_M vs $DU_G^3 (\rho_G \rho_L)^{1/2}$. The suggestion was motivated by the observation that a plot of this type (or a plot of E/E_M vs U_G) should show no effect of liquid flow rate if R_A varies linearly with the excess film flow and linearly with W_{LE}/Q_G. The spread of the measurements in figures 11–13 reflects the observation that the deposition constant k, defined by [4], decreases with increasing liquid flow.

The plot suggested by Dallman *et al.* was based on data from small-diameter pipes for which R_A appears to vary with U_G^2, rather than with U_G. The measurements presented in this paper therefore suggest that $DU_G^2 (\rho_G \rho_L)^{1/2}$ would be a better variable with which to correlate E/E_M.

Asali *et al.* (1985a) used the Dallman *et al.* (1979) method for correlating the entrainment measurements obtained (in the same equipment used in this study) by measuring local values of the liquid flux with a sampling tube. The results shown in figures 11–13 are consistent with Asali *et al.*'s measurements in that they show an increase in E/E_M with increasing pipe diameter. This is interpreted by the observation that the deposition constant, k, defined by [4], decreases with increasing pipe diameter. The dashed curves in figures 11–13 were calculated using the relation $R_A = R_D$ and by defining R_D by [30]. It is noted that this presents a lower limit of the measurements of E/E_M. The solid curves were calculated by using an equation of the form of [12] with values of k that give average fits of all the measurements in figures 8–10, and not just the measurements for small W_{LE}.

Finally, it should be noted that the entrainment measurements presented in this paper are consistently lower than those presented by Asali *et al.* (1985a). This is not understood and appears to be associated with differences in the techniques that were used. The device used by Asali *et al.* to sample gas flow was an impact tube with a beveled end. Its inside diameter was 3.175 mm and its thickness was 0.794 mm. The local droplet flux was calculated as the ratio of the mass flow of the liquid to the inside area of the impact tube. These local fluxes were integrated to obtain the total flux. A possible source of error is the definition of the effective sampling area. For example, if the effective diameter were 10% larger than the actual inside diameter, then the entrainment measurements from the two investigations would be in better agreement.

Another (and, perhaps, a more important) source of error is that local fluxes could not be measured too close to the liquid film because the tube would sample the tops of roll waves. The calculation of the total flux therefore involved an extrapolation of local flux measurements to the interface. Asali *et al.* (1985a) estimated that this extrapolation could cause a maximum error of 18%.

Because of the uncertainties associated with sampling tube measurements it is believed that the entrainment results given in this paper are more reliable.

Acknowledgements—This work was supported by Grant NSF CBT-85-19098, by the Shell Companies Foundation and by the Department of Energy under Grant DEF G02-86ER13556.

REFERENCES

ABOLFADL, M. & WALLIS, G. B. 1985 A mixing length model for annular two phase flow. *Physicochem. Hydrodynam.* **6**, 49–68.

ANDREUSSI, P. 1983 Droplet transfer in two-phase annular flow. *Int. J. Multiphase Flow* **9**, 697–713.

ANDREUSSI, P. & AZZOPARDI, B. J. 1983 Droplet deposition and interchange in annular two-phase flow. *Int. J. Multiphase Flow* **9**, 681–695.

ANDREUSSI, P. & ZANELLI, S. 1976 Liquid phase mass transfer in annular two-phase flow. *Ingegn. chim.* **12**, 132–136.

ANDREUSSI, P. & ZANELLI, S. 1979 Downward annular and annular-mist flow of air–water mixtures. In *Two-phase Momentum, Heat and Mass Transfer*, Vol. 2 (Edited by DURST, F., TSIKLAURI, G. V. & ALGAN, N. H.). Hemisphere, Washington, D.C.

ANDREUSSI, P., ASALI, J. C. & HANRATTY, T. J. 1985 Initiation of roll waves in gas–liquid flows. *AIChE Jl* **31,** 119–126.

ANDRITSOS, N. 1986 Effect of pipe diameter and liquid viscosity on horizontal stratified flow. Ph.D. Thesis, Univ. of Illinois, Urbana.

ASALI, J. C. 1984 Entrainment in vertical gas–liquid annular flow. Ph.D. Thesis, Univ. of Illinois, Urbana.

ASALI, J. C., LEMAN, G. W. & HANRATTY, T. J. 1985a Entrainment measurements and their use in design equations. *Physicochem. Hydrodynam.* **6,** 207–221.

ASALI, J. C., HANRATTY, T. J. & ANDREUSSI, P. 1985b Interfacial drag and film height for vertical annular flow. *AIChE Jl* **31,** 895–902.

AZZOPARDI, B. J. 1988 The role of drops in annular gas–liquid flow; drop sizes and velocities. *Jap. J. Multiphase Flow* **2,** 15–36.

COUSINS, L. B. & HEWITT, G. F. 1968 Liquid phase mass transfer in annular gas–liquid two-phase flows: radia mixing. UKAEA Report AERE-R5693.

DALLMAN, J. C., JONES, B. G. & HANRATTY, T. J. 1979 Interpretation of entrainment measurements in annular gas–liquid flows. In *Two-phase Momentum, Heat and Mass Transfer*, Vol. 2 (Edited by DURST, F., TSIKLAURI, G. V. & AFGAN, N. H.), pp. 681–693. Hemisphere, Washington, D.C.

HEWITT, G. F. & HALL-TAYLOR, N. S. 1970 *Annular Two-phase Flow*. Pergamon Press, Oxford.

HEWITT, G. F., GILL, L. E. & LACEY, P. M. 1964 Sampling probe studies of the gas core in annular two-phase flow, part 2. Studies of the effect of gas phase flow rates on phase and velocity distribution. *Chem. Engng Sci.* **19,** 665–682.

HINKLE, W. D. 1967 A study of liquid mass transport in annual air–water flow. Sc.D. Thesis, MIT, Cambridge, Mass.

LEE, M. M., ADRIAN, R. J. & HANRATTY, T. J. 1989 The interpretation of droplet deposition measurements with a diffusion model. *Int. J. Multiphase Flow* **15,** 459–469.

LEMAN, G. W. 1985 Atomization and deposition in two-phase annular flow: measurement and modelling. Ph.D. Thesis, Univ. of Illinois, Urbana.

LEMAN, G. W., AGOSTINI, M. & ANDREUSSI, P. 1984 Tracer analysis of developing two-phase annular flow. *Physicochem. Hydrodynam.* **6,** 223–237.

MOECK, E. O. & SLACHIEWICZ, J. W. 1972 A droplet interchange model for annular–dispersed two phased flow. *Int. J. Heat Mass Transfer* **5,** 637–653.

NAMIE, S. & UEDA, T. 1972 Droplet transfer in two-phase annular mist flow; Part 1, experiment of droplet transfer rate and distributions. *Bull. JSME* **15,** 1568–1580.

OWEN, D. G. & HEWITT, G. F. 1987 An improved annular two-phase flow model. Presented at the *3rd Int. Conf. on Multiphase Flow*, The Hague.

OWEN, D. G., HEWITT, G. F. & BOTT, T. R. 1985 Equilibrium annular flows at high mass fluxes; data and interpretation. *Physicochem. Hydrodynam.* **6,** 115–131.

QUANDT, E. R. 1965 Measurement of some basic parameters in two-phase annular flow. *AIChE Jl* **11,** 311–318.

SCHADEL, S. A. 1988 Atomization and deposition rates in vertical annular two-phase flow. Ph.D. Thesis, Univ. of Illinois, Urbana.

SCHADEL, S. A. & HANRATTY, T. J. 1989 Interpretation of atomization rates of the liquid film in gas–liquid annular flow. *Int. J. Multiphase Flow* **15,** 893–900.

TEIXEIRA, J. C., AZZOPARDI, B. J. & BOTT, T. R. 1987 The effect of inserts in drop sizes in vertical annular flow. UKAEA Report AERE R12641.

WOODMANSEE, D. E. & HANRATTY, T. J. 1969 Mechanism for the removal of droplets from a liquid surface by a parallel air flow. *Chem. Engng Sci.* **24,** 299–307.